Th P10 12

2D Waveform Inversion for Near Surface Characterization - Application to a Land Dataset from Saudi Arabia

T.L. Tonellot* (Saudi Aramco), S. Operto (Geoazur), R. Brossier (ISTerre) & J. Virieux (ISTerre)

SUMMARY

Full seismic waveform inversion is an iterative data fitting procedure, based on full waveform modelling, which directly extracts high resolution quantitative information on the subsurface from seismograms. We present an application of frequency-domain early arrival acoustic waveform inversion to a 2D land seismic dataset in Saudi Arabia for near-surface velocity model building. Traditional traveltime methods for velocity estimation can be inadequate in arid environments where karsting, low velocity layers, outcropping refractors, and strong velocity contrasts are common. We show that the velocities estimated by waveform inversion dramatically improve the imaging of nearsurface structures compared to traveltime tomography.

Introduction

Successful seismic imaging of low relief structures and stratigraphic traps in arid land environments strongly depends on how accurately velocities in the first 500 m to 700 m of the subsurface are known. Sand dunes, topography, karsted carbonates, dry river beds, outcropping refractors, velocity reversals, anhydrites, and layered basalts are some of the many "features" contributing to the complexity of the Saudi Arabian near-surface (Keho, 2011). These features have a complicating and often degrading effect on signal penetration, trace amplitudes and near-surface velocities. This complexity in the near-surface is commonly addressed with standard tools like single-layer and multi-layer velocity models, refraction statics and tomostatics methods (Bridle et al., 2007).
Thanks to a more accurate representation of wave propagation physics, waveform inversion has the potential to deliver higher resolution velocity models compared to the ones obtained with traveltime-based technologies (Virieux and Operto, 2009). Many publications have demonstrated this potential on synthetic and/or marine data (Sirgue et al., 2009). Applications to land data are still very limited and challenging, mainly due to data quality and mostly restricted to 2D data with very large offsets (Malinowski et al., 2011; Plessix et al., 2010).
In this paper, we present an application of waveform inversion to 2D land data in Saudi Arabia. A frequency domain waveform inversion algorithm is used. The seismic data are preconditioned to remove ambient noise and surface waves. Depth migrated images using traveltime and waveform inversion velocities are generated and compared.

Waveform inversion method

We use a visco-acoustic waveform inversion algorithm implemented in the frequency domain (Malinowski et al., 2011). Acoustic wave propagation modelling is performed by a finite-difference method in the frequency space domain. Solving the frequency domain full wave equation by finite difference reduces to solving a large sparse linear system whose so-called impedance matrix depends on frequency and model parameters and whose righthand side vector represents the seismic source. A parallel direct factorization method (Amestoy et al., 2001) is used to solve the system.
Waveform inversion is achieved by minimizing an L2 norm in the data space, measuring the misfit between the modelled and observed data with a preconditioned steepest descent algorithm. The gradient is scaled with the diagonal elements of the approximate Hessian matrix and smoothed with an adaptive 2D Gaussian filter. The inversion starts from an initial low frequency model computed by traveltime tomography. Nonlinearities are efficiently mitigated by adopting a multi-scale strategy in which higher wave numbers are progressively incorporated in the model by sequential inversion of increasing frequency. The model obtained at a given frequency is used to start the inversion of the next one.

Application to land data

The dataset under consideration is a 9,000 m seismic line consisting of 716 shots with 716 receivers per shot. The shot and receiver intervals are both 12.5 m. The maximum offset per shot is 8,950 m. A standard pre-processing sequence, including surface consistent scaling and filtering in the FK domain, was applied to the data to remove ambient noise, surface waves and anomalous amplitudes. Figures 1 and 2 show the result of this pre-processing on a typical shot located in the middle of the line. Note the strong reflections in the upper half of this shot.
Due to data quality and to the presence of shingling, the first breaks were not picked beyond the 1,500 m offset. An initial model was built by first arrival traveltime tomography (Zhang and Toksoz, 1998). This model, which is shown in Figure 3, fits the picked traveltimes with a RMS residual of 23 ms. A synthetic dataset was computed in the initial model with a Dirac source wavelet, a maximum frequency of 20 Hz, and no attenuation (Q=10,000). A source wavelet was then computed for each shot gather in the time domain following the approach described in Pratt et al. (1999). Synthetic data that can be compared to the recorded ones were then obtained by convolution of the Dirac synthetic shot gathers with the extracted source wavelets. This comparison led to the selection of the offset range of 500 m to 2,000 m for the remainder of the study. Indeed, offsets lower than 500 m in the

recorded data were contaminated by surface wave residuals; and beyond the 2,000 m offset, the velocities from the starting model were too inaccurate.

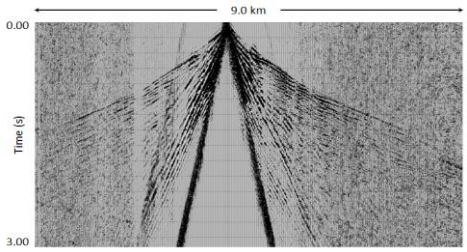

Figure 1: Raw shot gather number 322 displayed with trace maximum normalization. Note the surface wave and ambient noise.

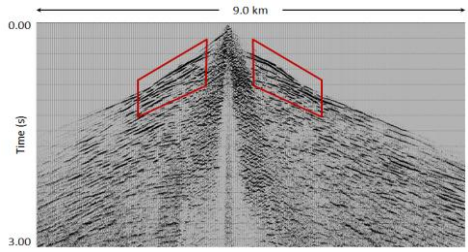

Figure 2: Shot gather number 322 after preconditioning displayed with trace maximum normalization. Red boxes show the offsets used for inversion.

One of the main pitfalls with early arrival waveform inversion of land data is related to the amplitude variation with offset of the recorded data, which is often quite different from modelled data. These differences, which can be attributed to attenuation and/or differences in radiation patterns between the recorded data and the acoustic approximation used to generate the synthetic data, are usually addressed with an ad-hoc scaling strategy, such as the ones described in Brenders and Pratt (2007) and Shen (2010). Figures 4 and 5, respectively, show the recorded and synthetic data in the initial model with a mute applied to preserve only the very first arrival. We found that the RMS amplitude variations with offset for these two datasets were very comparable, as shown in Figure 6. No scaling strategy was therefore required and given that the synthetic data was generated with a high Q factor, we concluded that an acoustic approximation was sufficient for this study.

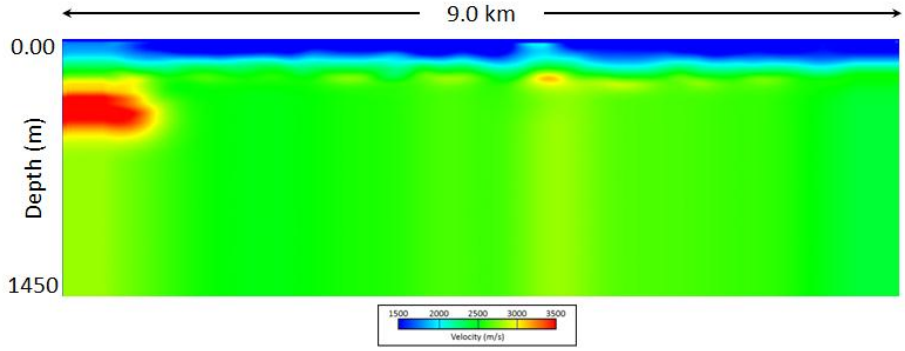

Figure 3: Acoustic velocity model built by first break traveltime tomography.

Figure 7 shows the early arrival data prepared for waveform inversion. A mute was applied to the preconditioned data to preserve the early arrivals, and only the shots with maximum offsets greater than or equal to 2,000 m were considered (a total of 501 shots).

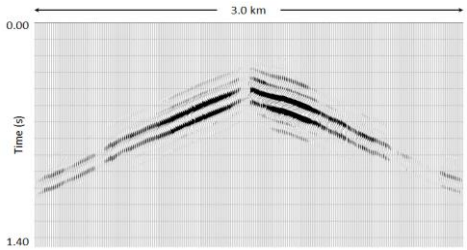

Figure 4: Preconditioned shot gather with a mute centered on the first arrivals. Offsets range from 500 to 2,000 m.

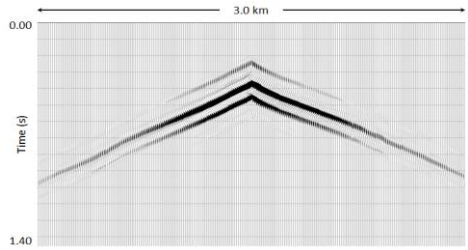

Figure 5: Synthetic shot gather with a mute centered on the first arrivals. Offsets range from 500 to 2,000 m.

Ten frequencies from 5 Hz to 20 Hz were sequentially inverted, with 15 iterations per frequency. The objective function decreased by 25% per frequency in average. During the waveform inversion a single source wavelet is estimated for all the shots. The resulting velocity model is shown in Figure 8. It reveals low velocity anomalies in the very near surface and a succession of high velocity layers, which were not present in the traveltime tomography model. In the absence of shallow borehole measurements, a way to quality control the full waveform inversion results consists in comparing synthetic and observed waveforms. Figure 9 displays the observed and synthetic traces in the initial and in the final waveform inversion models.

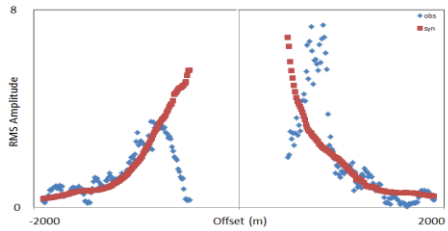

Figure 6: First arrivals RMS amplitude variation with offset for the observed (blue) and synthetic (red) data at the same shot in Figure 5.

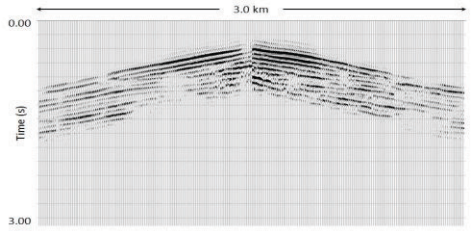

Figure 7: Windowed preconditioned data used as input for the waveform tomography. Offsets range from 500 to 2,000 m.

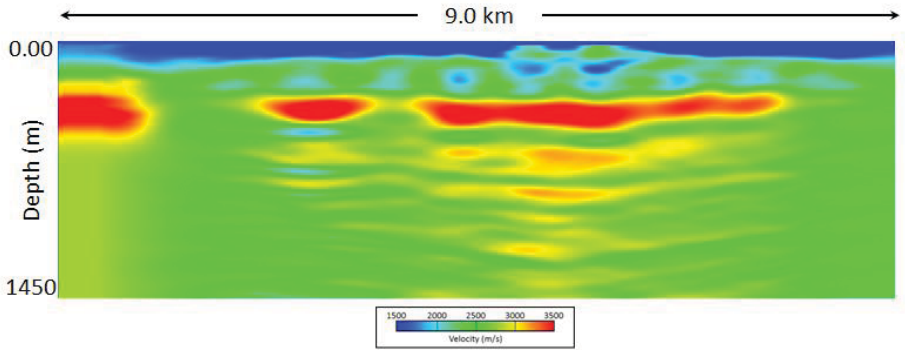

Figure 8: Waveform inversion result.

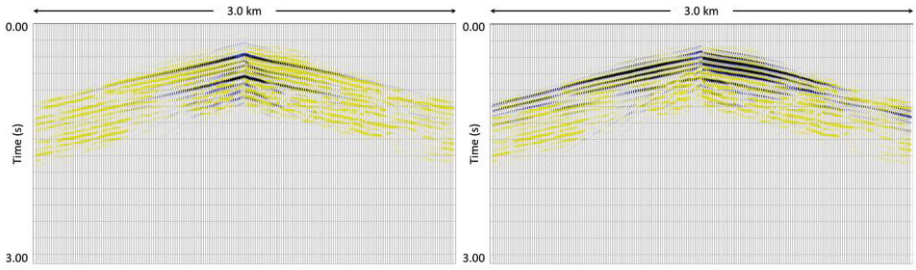

Figure 9: Comparison between synthetic (blue) and recorded (yellow) shot gather at iteration 1 (left) and 15 (right). Black color corresponds to common parts.

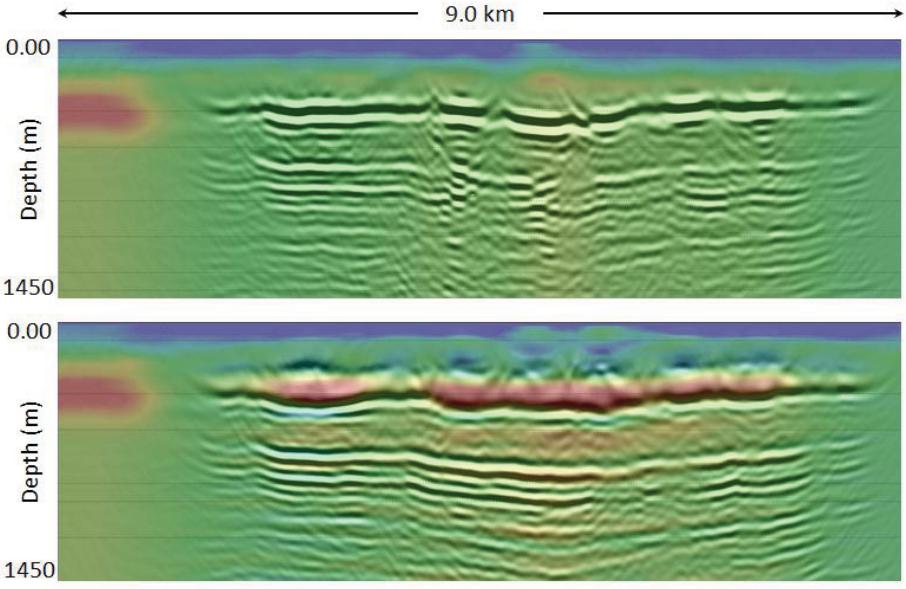

Figure 10: Depth-migrated images comparison with initial (top) and final (bottom) velocity models. The velocity models are shown in the background.

The waveform inversion has clearly improved the overall fit of the first arrivals and it was able to partially reconstruct the reflected arrivals included in the inverted time window, which correspond to the high velocity layers present in the waveform inversion model.

To further assess the quality of the model reconstructed by waveform inversion, we depth-migrated the preconditioned data — using both the initial traveltime tomography model and the waveform inversion model — with a phase-shift-plus-interpolation algorithm (Fei and Liu, 2006). The corresponding images are shown in Figure 10. The waveform inversion velocity model provides a much more focused and coherent image with fewer migration artefacts compared to the traveltime model.

Conclusions

We compare a near-surface model derived from acoustic early arrival waveform inversion to a model derived by traveltime tomography for a 2D survey in Saudi Arabia. The waveform inversion produces a velocity model revealing significant differences when compared to traveltime inversion. The validity of the waveform inversion velocity model is confirmed both by a better fit of the synthetic with observed waveforms and by an improved depth image compared to the traveltime inversion. This study illustrates the potential for waveform inversion to improve near surface reconstruction in arid environments.

Acknowledgments

The authors would like to thank Saudi Aramco for permission to publish this paper and Tong Fei, Robert Ley and Joe McNeely from Saudi Aramco.

References

Amestoy, P.R., Duff, I.S. and L'Excellent, J.-Y., 2001, A fully asynchronous multifrontal solver using distributed dynamic scheduling, SIAM Journal of Matrix Analysis and Appli., 23, 1, 15-41.
Brenders, A.J. and Pratt, R.G., 2007, Efficient waveform tomography for lithospheric imaging: Implications for realistic 2D acquisition geometries and low frequency data: Geophys. J. Int., 168, 152-170.
Keho, T.H., 2011, Near Surface Challenges for Processing 3D Seismic, 73rd EAGE Conference & Exhibition - WS2.
Bridle, R., Ley, R. and Al Mustafa, A., 2007, Near-surface models in Saudi Arabia, Geophysical Prospecting, 55, 779-792.
Fei, T.W. and Liu, Q., 2006, Wave Equation Migration for 3D VSP Using Phase-shift Plus Interpolation, 76th SEG Expanded Abstracts.
Malinowski, M., Operto, S. and Ribodetti, A., 2011, High-resolution seismic attenuation imaging from wide-aperture onshore data by visco-acoustic frequency-domain full-waveform inversion, Geophys. J. Int., 186, 1179-1204.
Plessix, R.-E., Baeten, G., de Maag, J.W., Klaassen, M., Rujie, Z. and Zhifei, T., 2010, Application of acoustic full waveform inversion to a low-frequency large-offset land data set, SEG Expanded Abstracts, 29, 930, DOI:10.1190/1.3513930.
Pratt, R.G., 1999, Seismic waveform inversion in the frequency domain, Part 1: Theory and verification in a physical scale model, Geophysics, 64, 888-901.
Shen, X., 2010, Near-surface velocity estimation by weighted early arrival waveform inversion: 80th SEG Expanded Abstracts, 1975-1979.
Sirgue, L., Barkved, O.I., Van Gestel, J.P., Askim, O.J. and Kimmedal, J.H., 2009, 3D Waveform Inversion on Valhall Wide-azimuth OBC, 71st EAGE Conference & Exhibition, EAGE, Expanded Abstract, U038.
Virieux, J. and Operto, S., 2009, An overview of full-waveform inversion in exploration geophysics, Geophysics, 74, WCC1.
Zhang, J. and Toksoz, N., 1998, Nonlinear refraction traveltime tomography, Geophysics, 63, 1726, DOI:10.1190/1.1444468.